

PROCEEDINGS OF SPIE

[SPIDigitalLibrary.org/conference-proceedings-of-spie](https://spiedigitallibrary.org/conference-proceedings-of-spie)

Wide-field spectroscopic imaging of biological-substance distributions on entire faces by measuring middle infrared lights emitted from human bodies itself

Suzuki, Yo, Qi, Wei, Fujiwara, Masaru, Hiramatsu, Hiroyuki, Suzuki, Satoru, et al.

Yo Suzuki, Wei Qi, Masaru Fujiwara, Hiroyuki Hiramatsu, Satoru Suzuki, Pradeep Abeygunawardhana, Kenji Wada, Akira Nishiyama, Ichiro Ishimaru, "Wide-field spectroscopic imaging of biological-substance distributions on entire faces by measuring middle infrared lights emitted from human bodies itself," Proc. SPIE 8951, Optical Diagnostics and Sensing XIV: Toward Point-of-Care Diagnostics, 89510Z (28 February 2014); doi: 10.1117/12.2038837

SPIE.

Event: SPIE BiOS, 2014, San Francisco, California, United States

Wide-field spectroscopic imaging of biological-substance distributions on entire faces by measuring middle infrared lights emitted from human bodies itself

Yo SUZUKI^a, Wei QI^a, Masaru FUJIWARA^a, Hiroyuki HIRAMATSU^a, Satoru SUZUKI^a, Pradeep Abeygunawardhana^a, Kenji WADA^b, Akira NISHIYAMA^b, Ichirou ISHIMARU^{*a}

^aDept. of Intelligent Mechanical Systems Engineering, Faculty of Engineering, Kagawa University, 2217-20 Hayashi-cho, Takamatsu, Kagawa-pref., 761-0396, Japan; ^bFaculty of Medicine, Kagawa University, 1750-1 Miki-cho, Kita, Kagawa-pref., 761-0793, Japan

ABSTRACT

We are aiming at the realization of the measurement technology for the biological-substance distributions, such as sebum, on entire faces at the daily-life environment. We proposed the imaging-type 2-dimensional Fourier spectroscopy [1] that is the palmtop-size portable measurement apparatus and has the strong robustness for mechanical vibrations. And the proposed method can measure the wide-field 2-dimensional middle-infrared spectroscopic-imaging of radiation lights emitted from human bodies itself without light sources. In the proposed method, we install the phase-shifter, that can give an arbitrary phase difference for the half-flux of objective beams, at the optical Fourier transform plane of the infinity corrected optical system. The near-common-path interferometer that is a phase-shift interferometer between objective beams can be realized. In this proposed method, the emitted rays from each single-bright-point on measurement surfaces can interfere with each other. Thus, even if the middle infrared-lights from human bodies are the spatially incoherent light, we can acquire the interferograms at each pixel on an imaging array-device in accordance with the amount of phase shift as the 2-dimensional image-intensity changes. We demonstrated the feasibility of the middle infrared spectroscopic imaging of whole human faces without active illuminations.

Keywords: Fourier spectroscopy, Spectroscopic imaging, Wide-field, Middle infrared light, Biological-substance, Imaging FTIR, Hyperspectral imaging, Common-path interferometer

1. INTRODUCTION

We are aiming at the realization of the wide-field spectroscopic-imaging method that has high portability and secures high sensitivity for mid-infrared lights. Because the proposed imaging-type 2-dimensional Fourier spectroscopy is a near-common-path phase-shift interferometer, the strong robustness against mechanical vibrations achieves high portability. Based on the Fourier spectroscopy, the high light-use-efficiency makes the mid-infrared spectroscopic-imaging available.

For conventional spectroscopy, so-called hyper-spectral camera have low light-use-efficiency, because AOTF (Acousto-Optic Tunable Filters) or dispersive spectrometer extracts small amount of light intensity within narrow band of wavelength. Thus, hyper-spectral cameras become to be large and expensive, because extremely-high-sensitive imaging sensors like EMCCD (Electron Multiplying Charge Coupled Device) should be introduced. But for mid-infrared region, even if the photon energy of mid-infrared light is very weak, there is no extremely-high-sensitive array device whose quantum efficiency is corresponds to EMCCD. Therefore, for mid-infrared region, Fourier spectroscopy with highest light-use-efficiency is indispensable method. However, generally speaking, Michelson interferometer that is basic optical configuration of Fourier spectroscopy has weak robustness for mechanical vibrations. Commercially available FTIR-type hyper-spectral cameras are mounted on anti-vibration mechanism. Thus, the cost becomes to be extremely expensive over 1million USD. And, the weight of FTIR-type hyper-spectral camera is around 30 kg that is six times compared with AOTF type and dispersion type [2].

Furthermore, for conventional methods, the view angle is limited into around 10 degrees, because the various incident-angle to AOTF or grating, that corresponds to view angles, deteriorates the narrow band of wavelength. Thus, the conventional hyper-spectral cameras can't be applied to wide field of view like omnidirectional imaging essentially.

On the contrary, the proposed imaging-type 2-dimensional Fourier spectroscopy is a near-common path interferometer with strong robustness for mechanical vibrations. Because the proposed method can be constructed as simple optical

* ishmaru@eng.kagawa-u.ac.jp; phone +81-87-864-2325; fax +81-87-864-2369

configuration without anti-vibration mechanism, the palmtop-size spectroscopy whose price will be several 10 thousand USD can be realized.

At 2nd. chapter, we describe the near-common-path phase-shift interferometer between objective beams. At 3rd. chapter, the omnidirectional spectroscopic imaging was verified with spatial incoherent lights without structural illuminations. At 4th. chapter, we mention the mid-infrared spectroscopic sensitivity with which several μm differences of glycerin thickness were recognized from spectral absorbance. At 5th. chapter, we demonstrated the feasibility of mid-infrared spectroscopic imaging of radiation lights emitted from body heat.

2. IMAGING-TYPE 2-DIMENSIONAL FOURIER SPECTROSCOPY

Figure 1 shows the schematic optical diagram of the imaging-type 2-dimensional Fourier spectroscopy. We install the variable phase-shifter at the optical Fourier transform plane of the infinity optical system. The variable phase-shifter is consisted of two kinds of mirror. One is the movable mirror that is actuated by piezo electric device with high accuracy. Another one is the fixed mirror. The proposed Fourier spectroscopic imaging method is a wavefront division phase-shift interferometer between objective beams.

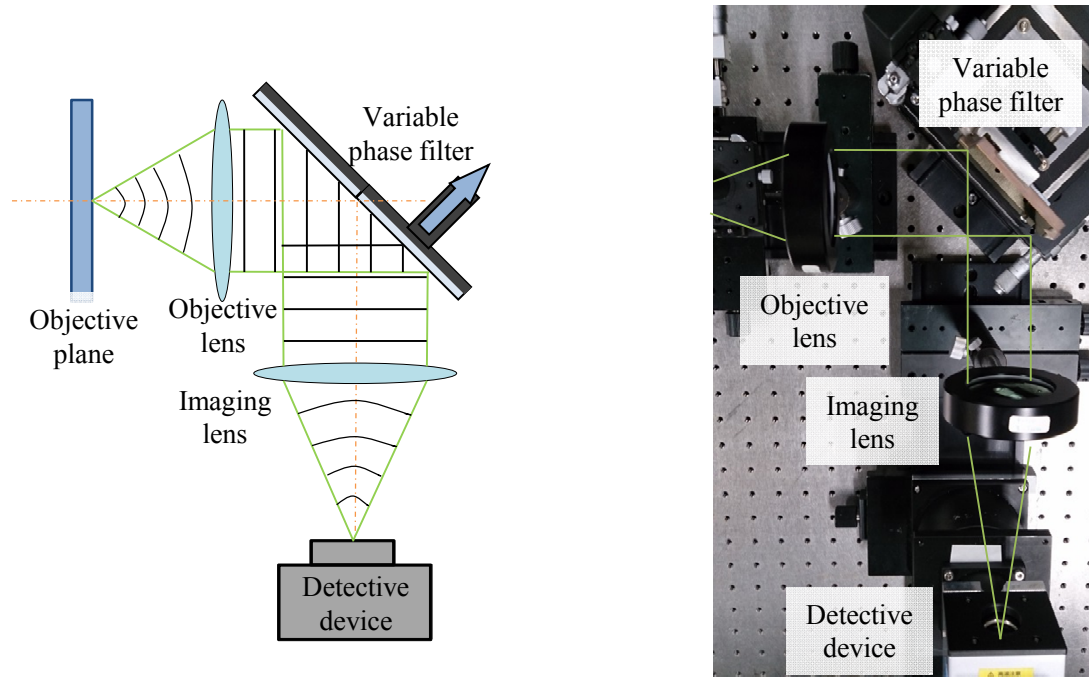
As shown in Fig. 1, from the optical point of view, objective surface is considered as bright-point aggregation. Rays emitted from single bright points are collimated by objective lens and concentrated into single points by imaging lens. Thus, conjugate bright points are formed on imaging plane. Each beam from multiple bright points on objective plane is concentrated into different plane-coordinates on 2-dimensional array device in accordance with field angles. Thus, the image is formed as 2-dimensional distributions of conjugate bright-points.

The variable phase-shifter gives an arbitrary phase difference at half flux of collimated objective rays. At an initial condition, the phases of every ray emitted from single bright points are equal and form the bright interference image. If half wavelength phase-difference is given to half flux of objective beams, two fluxes are interfered each other on imaging plane and weaken each other as interference phenomenon. In this case, the intensity of formed points becomes to be low. And then, if single wavelength difference is added to half flux of objective beams, two half fluxes are strengthen and form bright-points with high intensity. If we use monochromatic light as light source, the simple cosine waveform of interference-intensity changes is observed in accordance with the amount of phase-shift value. For spectroscopy, we use the polychromatic light as light source. For long wavelength components, cyclic changes of interference intensity become to be low frequency. Intensities of short wavelength components changes with high frequency. Sum of these multiple-cyclic interference-intensity-changes form the interferogram at every pixels simultaneously. As mentioned previously, because the interferogram consists of multi-frequency waveform, we can acquire the relative intensities at each frequency analytically by mathematical Fourier transform algorithm. As well-known as conventional Fourier spectroscopy, we can convert into spectroscopic characters that are the relative intensities at each wavelength by inverted value of frequency.

As previously explained, because all rays from single bright points are used for spectroscopy based on Fourier spectroscopy, the light-use-efficiency of the proposed method is quite high. And because the rays from single bright points are interfered, we can observe interference phenomena even if spatially incoherent lights like radiation heats. If we want to observe the wide field view for environmental measurements, such as earth observations, the object can't be illuminated actively. And to identify the substantial components from spectral absorbance, mid-infrared lights is suitable. The radiant lights emitted from objective heat itself are spatially incoherent light. And even if the photon energy of mid-infrared lights is very low, we can apply the proposed imaging-type 2-dimensional Fourier spectroscopy for radiation heat emitted from objective heat itself without structural illumination. Moreover, if a hyperboloidal mirror is installed as objective lens, we can obtain the omnidirectional Fourier spectroscopic imaging. And because of a near common path interferometer, the proposed method has strong robustness against mechanical vibrations and utilize the simple optical configuration. The palm-top size spectroscopic imager whose length is around 100mm on a side is available for daily life environmental sensor.

As shown in right-hand-side photo of Fig.1, the spectroscopic imager of mid-infrared radiation for wavelength region 8-14[μm] was constructed. The microbolometer (Maker: Nippon Avionics Co.,Ltd., Type:C100V) was used for imaging sensor. A microbolometer is a specific type of bolometer used as a detector in a thermal camera. The variable phase-shifter was actuated by piezoelectric device (Maker: PI, Type: P629). Because the focal length of objective lens and

imaging lens is equal ($f=100\text{mm}$, ϕ 50mm, material: Ge), the optical magnification is $1\times$. In 3rd. chapter, the omnidirectional spectroscopic setup for visible light is explained.



(a) Ray diagram of proposed method. (b) Overview of constructed optical setup of experimental apparatus.
 Figure 1 Schematic optical diagram of the imaging-type 2-dimensional Fourier spectroscopy in mid-infrared region.

3. OMNIDIRECTIONAL SPECTROSCOPIC IMAGE WITH VISIBLE LIGHT

Figure 2 shows the omnidirectional spectroscopic setup and experimental results. The optical setup is configured with 2 units. One is the spectroscopic imaging unit whose basic configuration is shown in Fig. 1. Another one is the conjugate-plane imaging unit. The spectroscopic imaging unit is the universal optical setup for varied application. The conjugate-plane imaging unit forms images on the objective plane of the spectroscopic imaging unit. Only by changing the objective lens of the conjugate-plane imaging unit, the optical magnification can be selectable. If a hyperboloidal mirror is install as objective lens of the conjugate-plane imaging unit, omnidirectional spectroscopic images can be obtained. In this experiment, we use the hyperboloidal mirror (maximum field angle: $50[\text{deg.}]$). And to form the whole omnidirectional view on the conjugate plane, the optical magnification of the conjugate-imaging unit was set to $0.15\times$. In this experiment, to demonstrate the feasibility of omnidirectional spectroscopy in visible lights, we used CCD (Charge Coupled Device) camera (Maker: SONY, Type: XC-77) for detective device. For the spectroscopic imaging unit, we set the focal length of objective lens and imaging lens equal ($f=100\text{mm}$, ϕ 35mm, material: BK7), because the optical apparatus can be made to be smaller. To secure the wavelength resolution 2.75nm , the stroke of phase-shift was $110\mu\text{m}$. To satisfy the sampling theory for short wavelength component $\lambda =400\text{nm}$, the movement resolution of piezoelectric device (Maker: PI, Type:P-622) was 91nm .

By observing the room that was illuminated by fluorescent ceiling lights s without structural illumination, we could confirm the changing of interference intensities on whole imaging-device area. From the analyzed spectroscopic characters, we could confirm the bright line spectra at $550[\text{nm}]$ (fluorescent substance: Tb) and $610[\text{nm}]$ (fluorescent substance: Eu). We could demonstrate the feasibility of omnidirectional spectroscopic imaging with spatial incoherent lights.

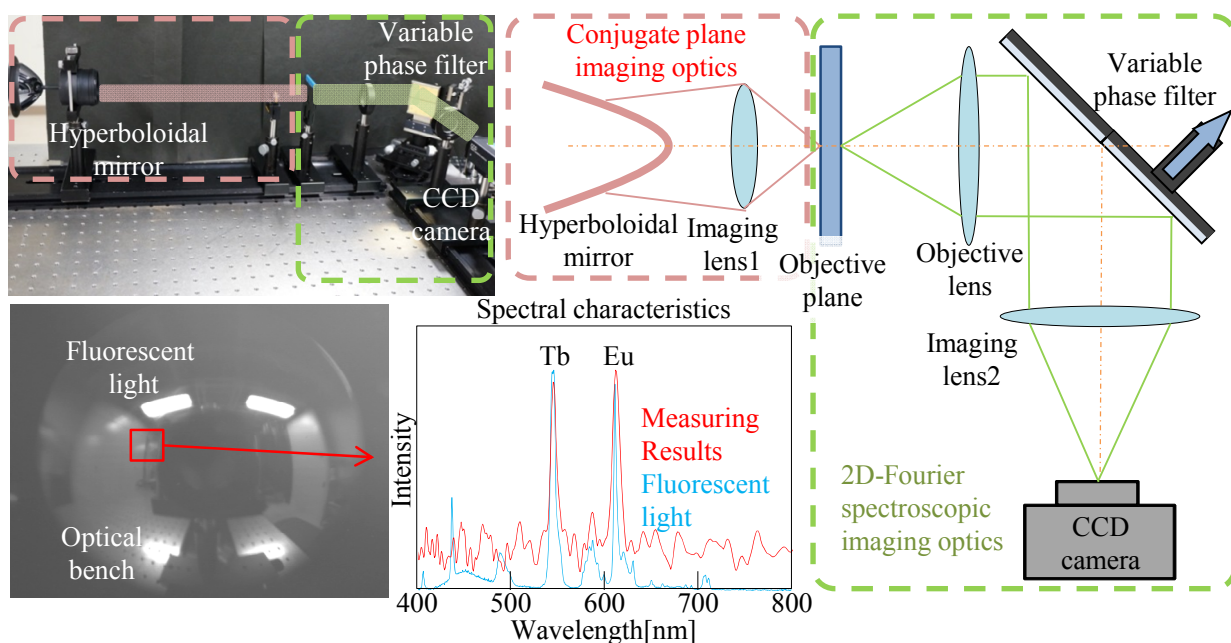


Figure 2 Experimental result of omnidirectional spectroscopic imaging with visible light.

4. EVALUATION OF IMAGING-TYPE 2-DIMENSIONAL FOURIER SPECTROSCOPIC IMAGING IN INFRARED REGION

4.1 Sensitivity evaluation of mid-infrared spectroscopic imaging using thin milk lotion layer

For mid-infrared region, the sensitivity of the proposed method was evaluated by measuring the minimum absorbance of thin μm -film. As shown in left-hand side photo of figure 3, 4 areas pasted with milky lotion (main ingredient: glycerin) on CaF_2 basal plate (area: $50 \times 50 \text{ mm}$, thickness: 2 mm) were used for the measurement sample. The area density of milky lotion of each area was $13 \mu\text{g}/\text{mm}^2$, $26 \mu\text{g}/\text{mm}^2$, $40 \mu\text{g}/\text{mm}^2$, $53 \mu\text{g}/\text{mm}^2$. First we measured masses of milky lotion by electric balances. Then the measured milky lotion were pasted over each area ($20 \times 20 \text{ mm}$) by hand work. If areas are evenly coated with milky lotion, the average thickness were estimated as $10.3 \mu\text{m}$, $20.6 \mu\text{m}$, $30.9 \mu\text{m}$, $41.2 \mu\text{m}$ based on the specific gravity of glycerin 1.26.

Using the experimental setup as shown in Fig.1, to observe the whole area of the basal plate, we set the optical magnification $0.025 \times$ of the conjugate imaging unit. To secure the wavelength resolution 57 nm , the stroke of phase-shift was 2.12 mm with sampling interval $1.41 \mu\text{m}$.

The left-hand side photo of Fig.3 shows the observed image of measuring sample in mid-infrared region. The transmission measurement of the basal plate by setting the black body whose temperature was 150°C as light source.

First, we compared with 4 spatial densities in each pasted area. We calculated averages of spectral absorbance in $20 \times 20 \text{ mm}$ area that was equivalent to 63×63 pixels. In the experimental results, averages of spectral-absorbance were increased with high spatial densities. The correlation between the absorbance at wavelength $9.6 \mu\text{m}$ and the averaged spatial density is shown in right lower side graph in Fig.3. Because the correlation coefficient was 0.9971, we could demonstrated that the extremely small amount of absorbance that was caused from thin $10 \mu\text{m}$ layer.

Next, to evaluate the unevenness within each pasted area, the merged area whose size was $3 \times 3 \text{ mm}$ was equivalent to 9×9 pixels. The evaluation results of thickness undulation is shown in upper side graph by calculating the averaged absorbance at wavelength $9.6 \mu\text{m}$ in each merged area. In the $13 \mu\text{g}/\text{mm}^2$ spatial-density area, the thickness at center was $16 \mu\text{m}$. And the thickness around pasted area was about $5\text{--}10 \mu\text{m}$ that was thinner than center thickness. And the thickness around edge of pasted area was $13 \mu\text{m}$ that was thicker than that of surrounding area. We assumed that because the milk lotion was dropped at the center of pasted area and spread into surrounding area, the thickness around center was thicker

than that of surrounding area. And because the milk lotion was gathered around edge of pasted area, the thickness was thicker again than that of surrounding area. We assumed that the unevenness of thickness distribution was corresponds to pasted process. In other pasted area the thickness around edge area was thicker than that of center area. We thought that because the amount of pasted milk lotion were high, the residual milky lotion were gathered around the edge of pasted area.

Milk lotion thickness were estimated from glycerin specific-gravity 1.26. The dispersion range of calculated milk-lotion-thickness are graphed as error bars in lower part of figure 4. The blue points indicate the average thickness in pasted area.

The left hand side graph in figure 4 shows the spectral absorbance measured by conventional FTIR. In accordance with spatial density of glycerin, we could confirm that overall spectral-waveform changed proportionally. The right lower side graph shows dispersions of estimated thickness of each glycerin spatial-density. Each error bar shows the range of maximum to minimum range of estimated thickness by proposed method. Blue marks indicate the estimated thickness of point measurement by FTIR. The point-measurement area was around 10mm×10mm. Red marks indicate the calculated average-thickness of pasted area from spatial thickness distributions as shown in Fig.4. The estimated thickness-distributions within 20mm square, what corresponds to error bars, include these two kinds of point measurement data. Thus, we validated the 2-dimensional spectral distribution of mid-infrared absorbance.

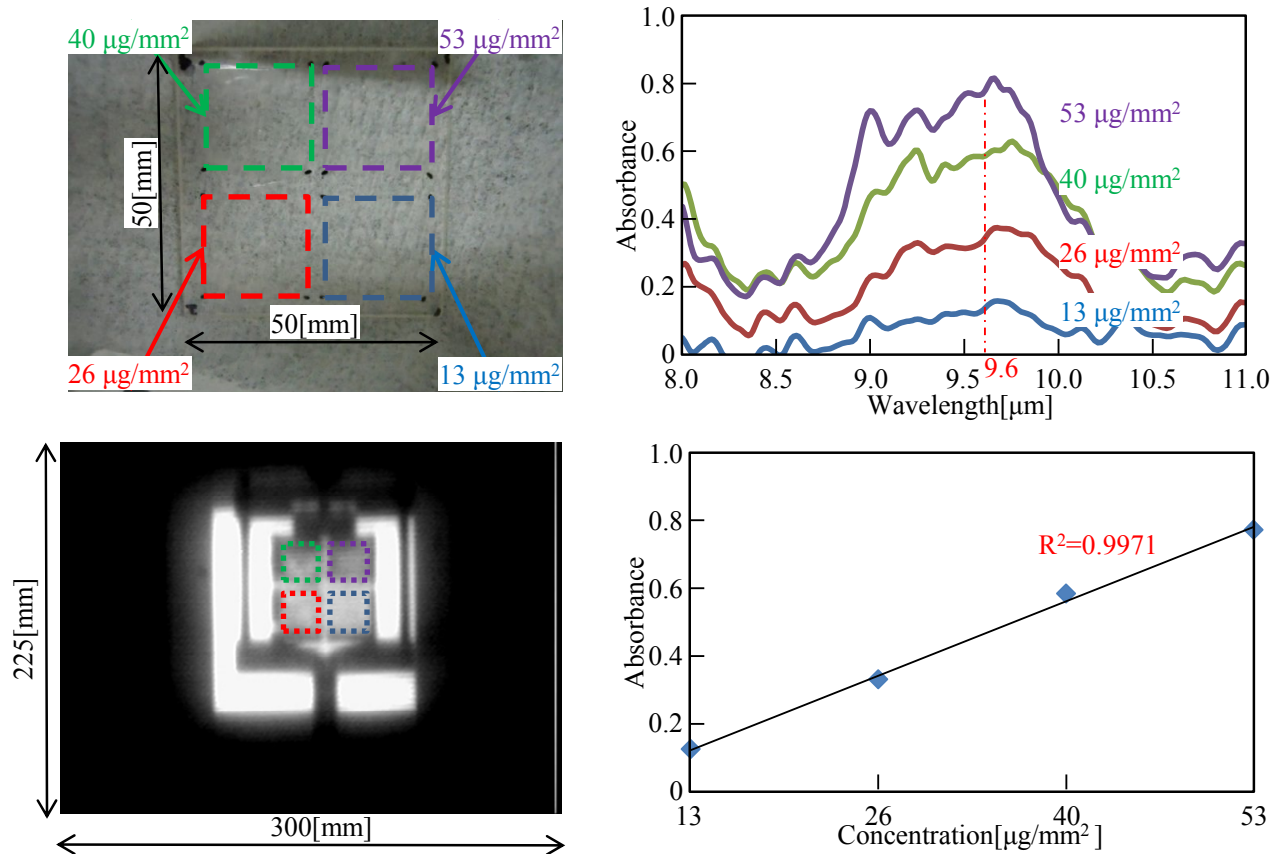


Figure 3 Measurement of the extremely small amount of absorbance that is caused by thin 10µm layer.

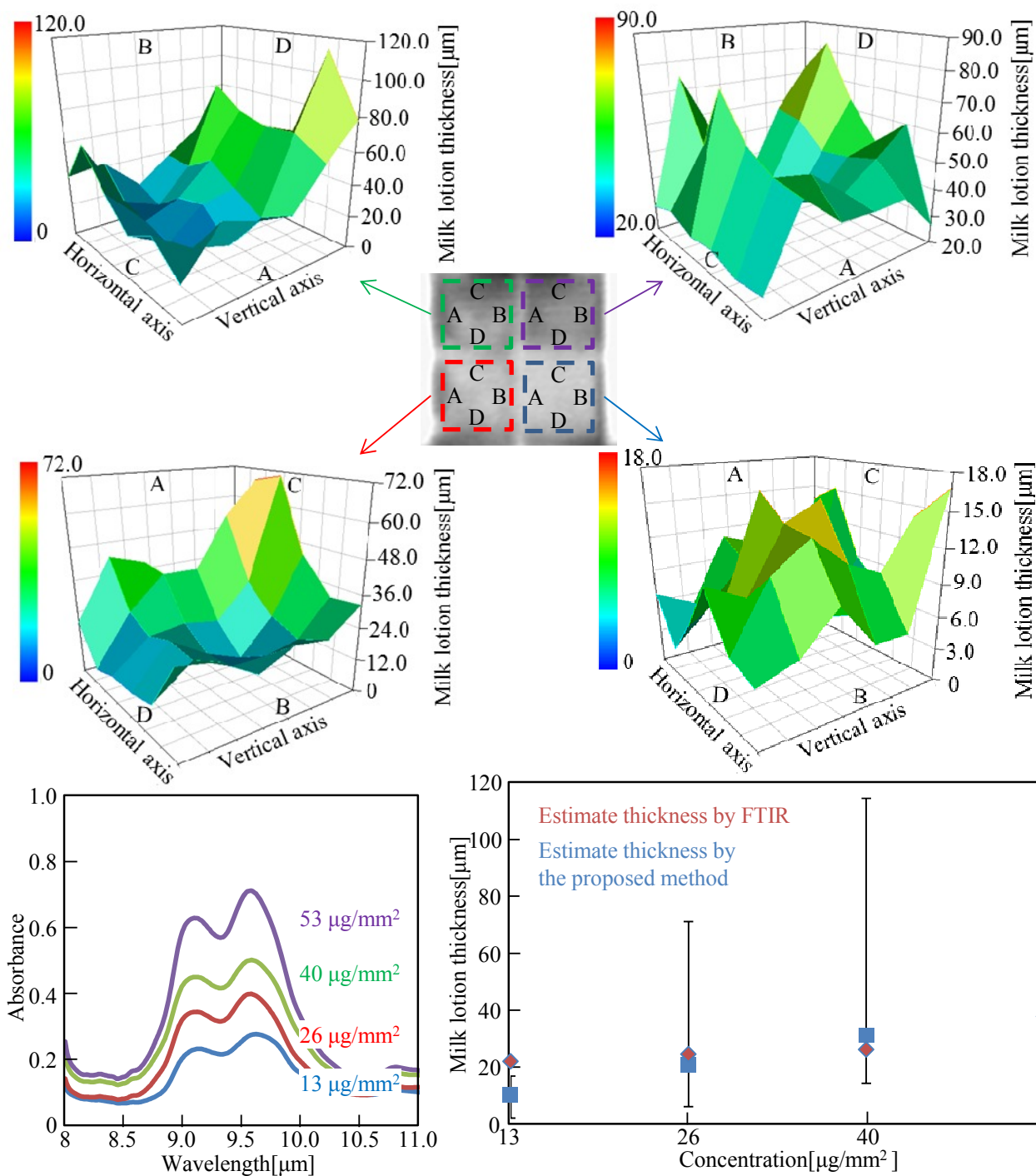


Figure 4 Visualization of the dispersion range of calculated milk-lotion-thickness and validity confirmation by conventional point-measurement with FTIR.

4.2 Wavelength accuracy evaluation using liquid cell in mid-infrared region

We evaluated the wavelength accuracy by measuring ethanol whose spectral characteristics are well known in near infrared region. In this evaluation, we used liquid cells whose windows material was BaF₂ (thickness: 2mm) and spacer thickness was 12 μ m. As the sample, we used the Japanese sake that includes ethanol and water. We set the optical magnification of the conjugate imaging unit 0.05 \times to observe whole area of the liquid cell. As shown in left upper side

graph shows in Fig.5, the transmission measurement with 150°C as light source. To secure the wavelength resolution 42nm , the stroke of phase-shift was 2.12mm and sampling interval was $1.41\mu\text{m}$.

The graph of spectral absorbance of conventional FTIR and proposed method is shown in lower side of figure 5. We could confirm that wavelengths of specific absorbance for ethanol and glucose are $9.3\mu\text{m}$, $9.6\mu\text{m}$, $11.5\mu\text{m}$. We could evaluate the accuracy within 42nm in wavelength axis.

For comparing the wavelength accuracy with the proposed method and FTIR, we evaluated the spatial distribution of absorbance at wavelength $9.6\mu\text{m}$ at 5-points of center and 4-surrounding areas. From the experimental results, the absorption-wavelength error at $9.6\mu\text{m}$ was $+15\text{nm}$ at center area. The error $+15\text{nm}$ was included within the theoretical wavelength resolution 42nm . At surrounding measurement areas, the error at left-hand-side was $+46\text{nm}$. The error at right hand side was -63nm . These errors at surrounding area were beyond the theoretical wavelength accuracy. We thought that these errors were caused from the wide view-angle. We also proposed the geometrical correction model for phase-shift value in accordance with angle of view [7].

Next, we evaluated the liquid-thickness distribution for liquid-cell area based on the absorbance at $9.6\mu\text{m}$. The spacer of liquid cell was $12\mu\text{m}$. As shown in upper-side graph in Fig.5, the evenness within $12\mu\text{m}\pm 2\mu\text{m}$ was confirmed. We can assume that the evenness of liquid-cell thickness may be relatively evenness compared with pasted milk-lotion. Thus, we could verify the wavelength accuracy that satisfies the designed value.

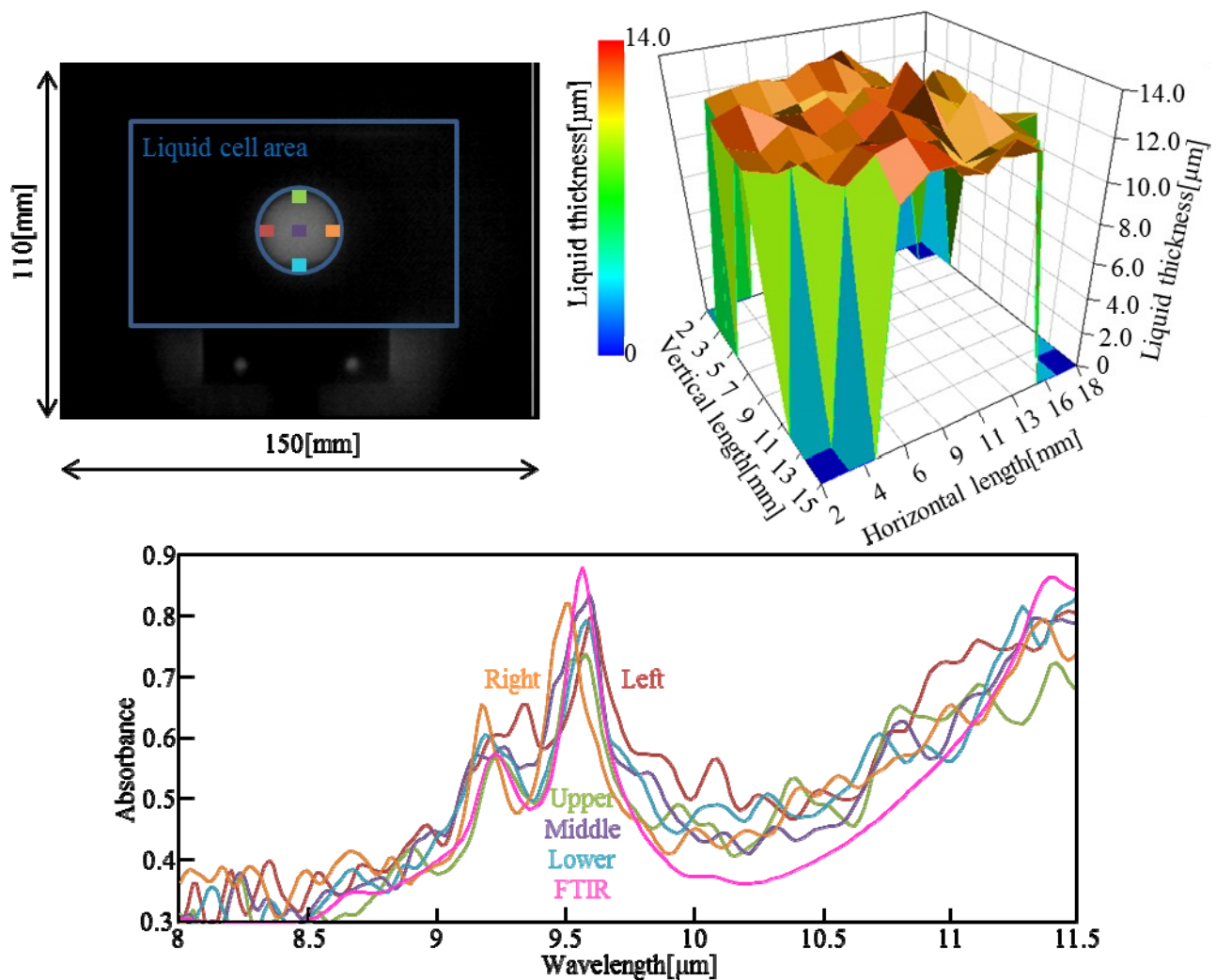


Figure 5 Wavelength-accuracy validation with evaluating the evenness of liquid-cell thickness from spectral absorbance distribution measured by the imaging-type 2-dimensional Fourier spectroscopy.

5. SPECTROSCOPIC IMAGING IN MID-INFRARED REGION OF RADIATION LIGHTS EMITTED FROM HUMAN BODIE'S HEAT ITSELF

We demonstrated the feasibility for measuring the spectral imaging of spatial incoherent lights and low photon energy in mid-infrared light that were emitted from human heat (temperature: around 300K). In this evaluation, to measure the whole face area, the optical magnification of conjugate imaging unit was set to 0.025 \times . Using the InSb camera (Maker: Nippon Avionics Co.,Ltd., Type: TVS-8500) , we observe the interference phenomena as shown in figure 6. We can observed the Fourier spectroscopic image without structural illumination. To secure the wavelength resolution 57nm, the stroke of phase-shift was 212 μ m, sampling interval was 707nm.

From the visualized distributions of interference intensities, we could recognize the high visibility of interference fringe of interferogram on a whole face area. As shown in right hand side graph of the interferogram on a part of face, we could demonstrate the feasibility of 2-dimensional spectral imaging in mid-infrared region.

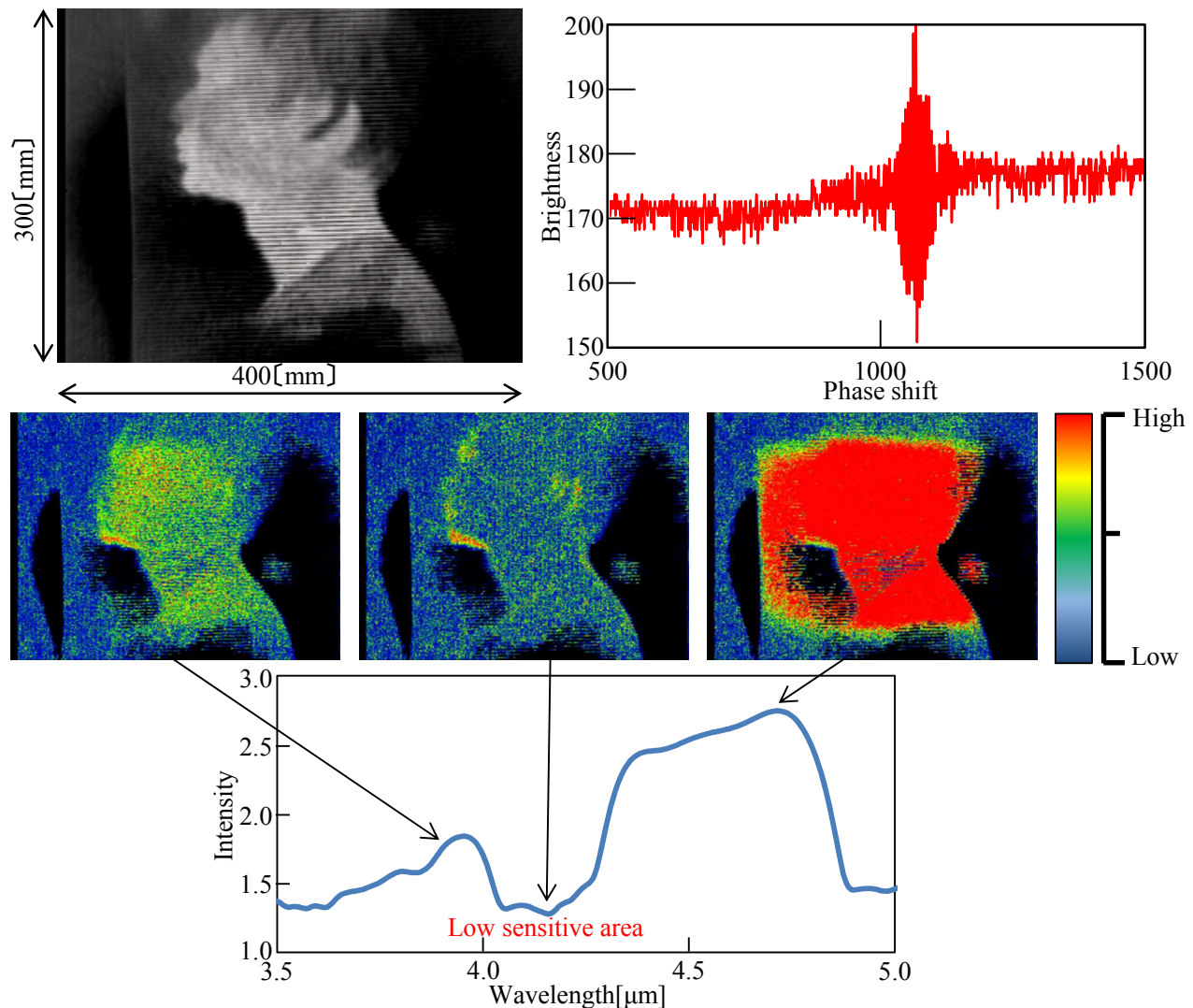


Figure 6 Feasibility demonstration of spectroscopic imaging in mid-infrared region of radiation lights emitted from human bodies heat itself.

6. CONCLUSION

We proposed the palm-top-size 2-dimensional Fourier spectroscopic imaging that can be used for daily life environment. We demonstrated the omnidirectional spectroscopic imaging of rooms illuminated by fluorescent ceiling lights without structural illuminations. And we evaluated the high sensitivity of our proposed method using the several μm thin layer of milk lotion. Moreover, the proposed method can visualize the dispersion of layer thickness. And we evaluated the wavelength accuracy using the spectral characteristics of ethanol. Finally, we demonstrated the feasibility of mid-infrared and wide-field spectroscopic imaging of human face by proposed palm-top size apparatus.

7. ACKNOWLEDGMENT

This project is supported by JST (Japan Science and Technology Agency) under the name of Development of Systems and Technology for Advanced Measurement and Analysis.

REFERENCES

- [1] Y. Inoue, I. Ishimaru, T. Yasokawa, K. Ishizaki, M. Yoshida, M. Kondo, S. Kuriyama, T. Masaki, S. Nakai, K. Takegawa, and N. Tanaka, "Variable phase-contrast fluorescence spectrometry for fluorescently stained cells", *Applied Physics Letters*, 89,121103 (2006)
- [2] Jean-Pierre Allard ; Martin Chamberland ; Vincent Farley ; Frédéric Marcotte ; Matthias Rolland, et al., "Airborne measurements in the longwave infrared using an imaging hyperspectral sensor", *Proc. SPIE 6954, Chemical, Biological, Radiological, Nuclear, and Explosives (CBRNE) Sensing IX*, 69540M (April 17, 2008);
- [3] Jaka Katrašnik ; Franjo Pernuš and Boštjan Likar, "Spectral characterization and calibration of AOTF spectrometers and hyper-spectral imaging system", *Proc. SPIE 7556, Design and Quality for Biomedical Technologies III*, 75560H (February 23, 2010)
- [4] Nathan Hagen and Michael W. Kudenov, "Review of snapshot spectral imaging technologies", *Opt. Eng.* 52(9), 090901 (Sep 23, 2013)
- [5] Daisuke Kojima ; Takashi Takuma ; Asuka Inui ; Wei Qi ; Ryosuke Tsutsumi, et al., "Spectroscopic tomography of biological tissues with the near-infrared radiation for the non-invasive measurement of the biogenic-substances", *Proc. SPIE 8229, Optical Diagnostics and Sensing XII: Toward Point-of-Care Diagnostics; and Design and Performance Validation of Phantoms Used in Conjunction with Optical Measurement of Tissue IV*, 82290M (February 1, 2012)
- [6] Wei Qi ; Takashi Takuma ; Asuka Inui ; Ryosuke Tsutsumi ; Takehiko Yuzuriha, et al., "The wide-field Fourier spectroscopic-imaging of the radiation heat from the object itself in the middle infrared region for the health monitoring", *Proc. SPIE 8229, Optical Diagnostics and Sensing XII: Toward Point-of-Care Diagnostics; and Design and Performance Validation of Phantoms Used in Conjunction with Optical Measurement of Tissue IV*, 82291A (February 1, 2012)
- [7] Asuka Inui, Ryosuke Tsutsumi, Wei Qi, Takashi Takuma, Hiroyasu KAGIYAMA Daisuke Kojima, Ichirou Ishimaru, "Correction Method of Phase Deference in Accordance with the Angle Field for Wide-Viewing-Angle Fourier-Spectroscopic-Imaging", *Physics Procedia*, Volume 19, 2011, Pages 61-66